New Journal of Physics
The open access journal at the forefront of physics
Deutsche Physikalische Gesellschaft DPG IOP Institute of Physics

PAPER • OPEN ACCESS

Universal phase transitions to synchronization in Kuramoto-like models with heterogeneous coupling

To cite this article: Can Xu *et al* 2019 *New J. Phys.* **21** 113018

IOP Publishing New J. Phys. 21 (2019) 113018 https://doi.org/10.1088/1367-2630/ab4f59

New Journal of Physics
The open access journal at the forefront of physics

Deutsche Physikalische Gesellschaft DPG
IOP Institute of Physics

Published in partnership with: Deutsche Physikalische Gesellschaft and the Institute of Physics

PAPER

OPEN ACCESS

RECEIVED
25 June 2019

REVISED
25 September 2019

ACCEPTED FOR PUBLICATION
18 October 2019

PUBLISHED
12 November 2019

Universal phase transitions to synchronization in Kuramoto-like models with heterogeneous coupling

Can Xu[1], **Stefano Boccaletti**[2,3], **Zhigang Zheng**[1] **and Shuguang Guan**[4]

[1] Institute of Systems Science and College of Information Science and Engineering, Huaqiao University, Xiamen 361021, People's Republic of China
[2] CNR-Institute of Complex Systems, Via Madonna del Piano, 10, I-50019 Sesto Fiorentino, Florence, Italy
[3] Unmanned Systems Research Institute, Northwestern Polytechnical University, Xi'an, 710072 People's Republic of China
[4] Department of Physics, East China Normal University, Shanghai 200241, People's Republic of China

E-mail: zgzheng@hqu.edu.cn and sgguan@phy.ecnu.edu.cn

Keywords: synchronization, Kuramoto model, phase transition

Abstract

We reveal a class of universal phase transitions to synchronization in Kuramoto-like models with both in- and out-coupling heterogeneity. By analogy with metastable states, an oscillatory state occurs as a high-order coherent phase accompanying explosive synchronization in the system. The critical points of synchronization transition and the stationary solutions are obtained analytically, by the use of mean-field theory. In particular, the stable conditions for the emergence of phase-locked states are determined analytically, consistently with the analysis based on the Ott–Antonsen manifold. We demonstrate that the in- or out-coupling heterogeneity have influence on both the dynamical properties (eigen'spectrum) and the synchronizability of the system.

1. Introduction

Synchronization of interacting units is a macroscopic self-organized behavior, and is ubiquitous in nature and human society. Examples range from physics, chemistry, engineering to social science [1], such as the flashing of fireflies, power grids, Josephon junction arrays, and neurons in human brain, etc [2, 3]. Synchronous evolutions are furthermore at the basis of cooperative functioning of many biological and man'made systems, and therefore revealing the mechanisms behind the setting and maintenance of synchronization is a very important issue [4].

The first prototypic model for investigating synchronization in coupled-phase oscillator was proposed by Winfree [5]. Later, Kuramoto refined the model, and made it mathematically tractable [6]. The classical Kuramoto model describes an ensemble of phase oscillators interacting via a sinusoidal function of the phase differences, and shows that a large population of oscillators can in fact synchronize despite the diversity in the individuals' natural frequencies. Such a pioneering work has inspired extensive studies on synchronization in the following four decades [7, 8]. Typically, synchronization in Kuramoto-like models turns out to be a continuous process, i.e. it follows a second-order phase transition. Recently, however, first-order-like synchronization transitions (the so called explosive synchronization) has also been revealed [9].

Besides the diversity in natural frequencies, heterogeneity in the coupling strength is also an important characteristic that may dominate in many real systems [10, 11], inducing the emergence of various coherent states in the route to synchronization, such as cardio-respiratory synchronization [12, 13] and network physiology studying networks between different organ systems [14–16]. Furthermore, non-local coupling is known as relevant for the formation of chimera states [17], and Kuramoto models with both positive and negative coupling can exhibit π states, travelling-wave states, standing-wave states, and glass states, among others [18, 19]. On the other hand, network structure leads to nontrivial phase transition, such as explosive synchronization [9] and cluster synchronization [20]. Recently, [21] shows that a metastable state appears in the route to the travelling-wave state near the hybrid phase transition, which has potential applications in the recover of human consciousness.

In this paper, we provide a comprehensive analysis for a system of coupled-phase oscillators by considering both in- and out-coupling heterogeneity. We characterize the dynamical behaviors in the system, and obtain the critical points of synchronization transition analytically. Remarkably, we show that the in- and out-coupling schemes have no influence on the critical point where the incoherent state becomes unstable, whereas synchronization ability is changed dramatically. A rigorous stability analysis for the phase-locked state is provided from different levels. We give a general condition for the stability of the phase-locked state based on the properties of eigen spectrum and the associated eigenvectors which are clarified. We reveal a universal route toward synchronization, i.e. from the incoherent state to the oscillatory state, then from the oscillatory state to the phase-locked state. Such route occurs even for purely attractive coupling, which is a signature that is different from the metastable state appearing near the hybrid phase transition.

The paper is organized as follow: in section 2 we introduce the dynamical model and the mean-field theory. In section 3 we focus on the stability analysis of the phase-locked state and its eigen-spectrum properties in detail. Section 4 provides a discussion about the tiered phase transition to the oscillatory state. Finally, conclusions are drawn in the last section.

2. Dynamical model and mean-field theory

Let us consider an ensemble of N intercating pase oscillators. The model we consider here has the form

$$\dot{\theta}_i = \omega_i + \sum_{j=1}^{N} K_{ij}\sin(\theta_j - \theta_i), \quad i = 1,\cdots,N, \tag{1}$$

where θ_i is the instantaneous phase of the ith oscillator, dot denotes temporal derivative, and ω_i is the natural frequency of the ith oscillator, which is taken from a specific distribution $g(\omega)$. N is the number of oscillators, and K_{ij} is the coupling value between the pair of oscillators i and j. In particular, $K_{ij} = \kappa/N(\kappa > 0)$ stands for the global and uniform coupling that is typically used in the Kuramoto model. In order to account for heterogeneity in the coupling, we set $K_{ij} = \kappa|\omega_i|/N$ or $K_{ij} = \kappa|\omega_j|/N$, which leads to a frequency-weighted Kuramoto model with $\kappa > 0$ [22, 23]. In the present study, we consider a uniform distribution

$$g(\omega) = \frac{1}{2\Delta}, \quad |\omega| < \Delta, \tag{2}$$

where Δ is the half-width of the distribution [24].

For the sake of convenience, we pay attention to the case of heterogeneity in the out-coupling, where $K_{ij} = \kappa|\omega_j|/N$, i.e. the weighted factor is inside the summation in equation (1). To characterize the collective behavior in the model

$$Z_1(t) = R(t)e^{i\Psi(t)} = \frac{1}{N}\sum_{j=1}^{N} e^{i\theta_j(t)} \tag{3}$$

is defined as the order parameter of the system, and

$$Z_2(t) = D(t)e^{i\Theta(t)} = \frac{1}{N}\sum_{j=1}^{N}|\omega_j|e^{i\theta_j(t)}, \tag{4}$$

which denotes the mean-field coupling of the system. The two complex vectors $Re^{i\Psi}$ and $De^{i\Theta}$ correspond to the centroid of the configurations $\{e^{i\theta_j}, \ |\omega_j|e^{i\theta_j}\}$. $D(t) = 0\,[R(t) = 0]$ denotes the incoherent state, where all oscillators are desynchronized and distribute uniformly on the unit circle. By applying the mean-field theory or linear stability analysis, one can obtain the critical coupling $\kappa_{c,1}$ for the onset of synchronization as

$$\kappa_{c,1} = \frac{2}{\pi|\Omega_c|g(\Omega_c)}, \tag{5}$$

where Ω_c is the critical mean-field frequency (the imaginary part of the eigenvalue), which satisfies the balanced principal-value integral equation [25]

$$P\cdot\int_{-\infty}^{\infty}|\omega|g(\omega)(\omega - \Omega_c)^{-1}d\omega = 0. \tag{6}$$

For the uniform distribution in equation (2), one has $\Omega_c = \pm\Delta/\sqrt{2}$ and $\kappa_{c,1} = 4\sqrt{2}/\pi$. Thus, the result is the same as the in-coupling case where $K_{ij} = \kappa|\omega_i|/N$. This suggests that the critical points for the emergence of synchronization in both out-coupling and in-coupling are the same [22].

Next, we seek for solutions of the coherent state. The dynamical equation (1) can be rewritten in the mean-field form as

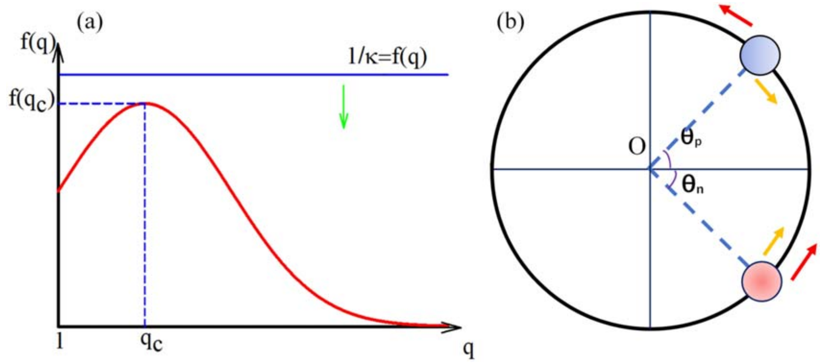

Figure 1. (a) Schematic plot of the self-consistent equation (13), $(q_c, f(q_c))$ is the maximum point of $f(q)$. (b) Schematic plot of the perturbation. θ_p and θ_n are a pair of symmetrical phase-locked oscillators with positive natural frequency, arrows stand for the perturbation directions. Red arrow is the even perturbation, and orange arrow is the odd perturbation.

$$\dot{\theta}_i = \omega_i - \kappa D \sin(\Theta - \theta_i). \tag{7}$$

In the long time limit ($t \to \infty$) the stationary solution of equation (7) indicates that D is independent of time and $\Theta = \Omega t$. Considering the symmetry of the system, we assume a rotating frequency $\Omega = 0$. Hence, the steady state for equation (7) is

$$\sin\theta_i = \frac{\omega_i}{\kappa D}, \quad |\omega_i| < \kappa D, \tag{8}$$

and

$$\cos\theta_i = \pm\sqrt{1 - \left(\frac{\omega_i}{\kappa D}\right)^2} \tag{9}$$

for the phase-locked oscillators. The drifting oscillators (with $|\omega_i| > \kappa D$) cannot be entrained by the mean-field and they rotate non-uniformly on the unit circle. It has been proved that the drifting oscillators have no contribution to the order parameter

$$D = \frac{1}{N}\sum_{|\omega_i|<\kappa D} |\omega_i| \cos\theta_i. \tag{10}$$

Letting N_ℓ be the number of phase-locked oscillators, there are 2^{N_ℓ} possibilities of configuration $\{\cos\theta_i\}$ except for those $D < 0$ in equation (10). However, if we perform an independent perturbation $\delta\theta_i$ for each locked phase θ_i, while keeping the others invariant, the corresponding eigenvalue equation is $\delta\dot{\theta}_i = \lambda\delta\theta_i$. The eigenvalue $\lambda = \frac{\partial\dot{\theta}_i}{\partial\theta_i}$, which yields

$$\lambda = -\kappa D\cos\theta_i + \frac{\kappa|\omega_i|}{N}\sin^2\theta_i. \tag{11}$$

The necessary condition for stable coherent state $D > 0$ requires all $\cos\theta_i > 0$.

As $N \to \infty$, the order parameter D should be re-defined in its integral form

$$D = \int_{\text{lock}} g(\omega)|\omega|\sqrt{1 - \left(\frac{\omega}{\kappa D}\right)^2}\,\mathrm{d}\omega. \tag{12}$$

Throughout the paper, we set $\Delta = 1$ for $\kappa D < 1$. The solutions are $D = 3\kappa^{-2}$ ($\kappa > 3$) and $R = 3\pi/(4\kappa)$ which correspond to partial synchronization. For $\kappa D > 1$, all oscillators become phase-locked. Setting $\kappa D = q$, equation (12) is transformed into

$$\frac{1}{\kappa} = f(q), \quad q > 1, \tag{13}$$

where $f(q) = \int_0^{1/q} qx\sqrt{1 - x^2}\,\mathrm{d}x$. Figure 1(a) plots the schematic function $f(q)$ ($q \geqslant 1$), and one can easily see that there is no intersection between $1/\kappa$ and $f(q)$ when κ is small enough. As κ increases, the line $1/\kappa$ is tangent to the curve $f(q)$ at $(q_c, f(q_c))$ and there are two solutions in the interval $\kappa \in (f(q_c)^{-1}, f(1)^{-1}]$. When $\kappa > f(1)^{-1} = 3$, there is only one solution that corresponds to a partial synchronization state. The critical point corresponding to the maximum of $f(q)$ is $q_c = (2/\sqrt{3})^{1/2}$, and the coupling strength that characterizes the emergence of completely phase-locked states is $\kappa_{c,2}^{\text{out}} = \frac{1}{f(q_c)} = 2\sqrt{1 + \frac{2}{\sqrt{3}}}$.

The situation for the in-coupling is relatively simple due to the symmetry. The system splits into two groups once $\kappa R > 1$, where $\cos\theta_i = \sqrt{1 - (\kappa R)^{-2}}$ and $\sin\theta_i = \pm(\kappa R)^{-1}$, and the choice of '±' is consistent with the sign of the natural frequency. The coherent solutions are $R_{\pm} = \frac{\sqrt{2}}{2}\sqrt{1 \pm \sqrt{1 - \frac{4}{\kappa^2}}}$, $\kappa \geqslant \kappa_{c,2}^{\mathrm{in}} = 2$, and they are independent on N and $g(\omega)$.

3. Stability of the phase-locked states

The above analysis shows that there are multi-branch solutions of the coherent state. Therefore, determining their stability becomes an important theoretical task. As we know, the incoherent state is neutrally stable due to the absence of eigenvalues for the linear operator in the region $\kappa < \kappa_{c,1}$, while its stability is further determined by the resonant pole calculated through analytical continuation [25]. The natural question is how the eigen-spectrum for the phase-locked state appears. In the following, we provide a detailed stability analysis of the coherent state for finite size N. We emphasize that the results can be straightforwardly extended to the case $N \to \infty$.

Choosing a pair of symmetric oscillators $\theta_{p,n}$ with opposite natural frequencies $\omega_{p,n}$, the governing equation of $\theta_{p,n}$ is

$$\dot{\theta}_{p,n} = \omega_{p,n} - \kappa(D_0 + D_1)\sin\theta_{p,n}, \tag{14}$$

where D_1 represents the local order parameter formed by $\theta_{p,n}$, $D_1 = (2|\omega_p|\cos\theta_p)/N$, and $D_0 = D - \mathrm{D}_1$ stands for the order parameter formed by the other $N - 2$ oscillators. Considering a special perturbation $\delta\theta_{p,n}$ that makes D_0 invariant, the linearized equation for $\delta\theta_{p,n}$ is governed by

$$\begin{pmatrix} \delta\dot{\theta}_p \\ \delta\dot{\theta}_n \end{pmatrix} = \begin{pmatrix} a - b & b \\ b & a - b \end{pmatrix}\begin{pmatrix} \delta\theta_p \\ \delta\theta_n \end{pmatrix}, \tag{15}$$

where $a = -\kappa D\cos\theta_p$ and $b = -(\kappa|\omega_p|\sin^2\theta_p)/N$.

The first eigenvalue of the Jacobian matrix is $\lambda_1 = -\kappa D\cos\theta_p$, which is always negative. The corresponding eigenvector satisfies $\delta\theta_p = \delta\theta_n$ representing identical perturbations, and it is stable. The second eigenvalue is $\lambda_2 = -\sqrt{(\kappa D)^2 - \omega_p^2} + 2\kappa|\omega_p|^3(\kappa D)^{-2}/N$, and the associated eigenvector satisfies $\delta\theta_p = -\delta\theta_n$ characterizing the perturbations in the reverse direction. As we will see, the two eigenvectors are the basis of the eigen-directions for general perturbations. When $\kappa D < 1$, $\lambda_2 > 0$ in the limit $|\omega_p| \to \kappa D$, and this implies that oscillators $\theta_{p,n}$ near the phase-locked boundary ($|\omega_p| \to \kappa D$) would first lose their stabilities under reverse perturbation (see figure 1(b)). Hence, one can conclude that the configuration where synchronous and drifting oscillators coexist is unstable.

A rigorous analysis needs to account for all perturbations $\delta\theta_i\,(i = 1, 2, \ldots, N)$ [26], then the linearized equation for phase-locked state is governed by

$$\delta\dot{\theta} = \mathbf{J}\delta\theta, \tag{16}$$

where $\delta\theta$ is a vector $(\delta\theta_1, \delta\theta_2, \ldots, \delta\theta_N)$ and $\mathbf{J}$ is the Jacobian matrix with entries $J_{ij} = \frac{\partial\dot{\theta}_i}{\partial\theta_j}$. For the out-coupling case

$$J_{ij} = \frac{\kappa}{N}|\omega_j|\cos(\theta_i - \theta_j) - \kappa D\cos\theta_i\delta_{ij}, \tag{17}$$

and $\kappa D > 1$. Note that $\sum_{j=1}^{N} J_{ij} = 0$, which implies that $(1, 1, \ldots, 1)$ is a trivial eigenvector corresponding to the eigenvalue $\lambda_1 = 0$. This property is associated with the rotation invariance of the Kuramoto model equation (1). Since $\mathbf{J}$ is a real and symmetric matrix, the stability condition for the phase-locked state is to have all other $N - 1$ eigenvalues $\lambda_i \leqslant 0\,(i = 2, 3, \ldots, N)$.

All detailed information about the eigen-spectrum comes from the characteristic equation of $\mathbf{J}$. To compute the characteristic polynomial, we express

$$\mathbf{J} = -\kappa D\mathbf{C} + \frac{\kappa}{N}\mathbf{MW}, \tag{18}$$

where $\mathbf{C}$ and $\mathbf{W}$ are the diagonal matrix with entries $\cos\theta_i$ and $|\omega_i|$ along the diagonal, respectively, and $\mathbf{M}$ is a real-symmetric matrix with elements $M_{ij} = \cos(\theta_i - \theta_j)$. Supposing $|\omega_i| > 0$, $\forall_i$, then

$$\lambda\mathbf{I} - \mathbf{J} = \lambda\mathbf{I} + \kappa D\mathbf{C} - \frac{\kappa}{N}\mathbf{MW} = \mathbf{E}\left(\mathbf{I} - \frac{\kappa}{N}\mathbf{E}^{-1}\mathbf{M}\right)\mathbf{W}, \tag{19}$$

and $\mathbf{E} = (\lambda\mathbf{I} + \kappa\,\mathrm{D}\mathbf{C})\mathbf{W}^{-1}$. Defining $\mathbf{c} = (\cos\theta_1, \cos\theta_2, \ldots, \cos\theta_N)$ and $\mathbf{s} = (\sin\theta_1, \sin\theta_2, \ldots, \sin\theta_N)$, the two vectors are linearly independent, i.e. $\mathbf{c}\cdot\mathbf{s} = 0$. Since the rank of $\mathbf{M}$ is only 2, for $\mathbf{x} \in \mathbf{R}^N$

$$\mathbf{Mx} = (\mathbf{c}\cdot\mathbf{x})\mathbf{c} + (\mathbf{s}\cdot\mathbf{x})\mathbf{s}. \tag{20}$$

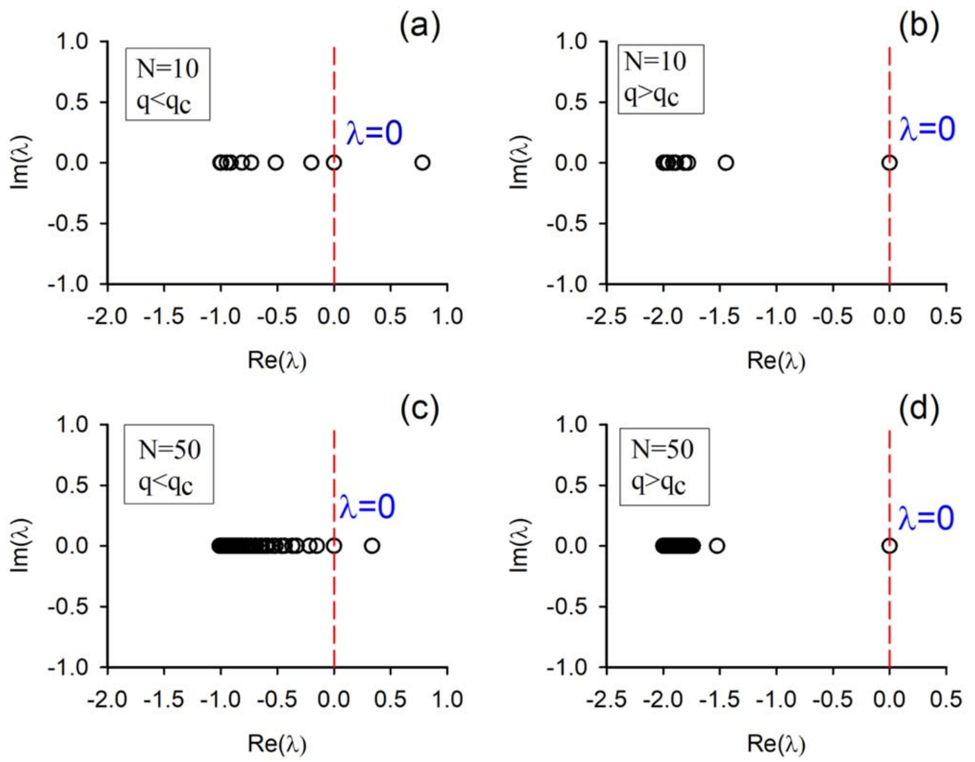

Figure 2. The eigen-spectrum of the Jacobian matrix **J** (see equation (17)). Panels (a) and (c) refer to $q = 1.01$ ($q < q_c$), for which the largest eigenvalue λ is positive; panels (b) and (d) refer to $q = 2.0$ ($q > q_c$), for which the largest eigenvalue λ vanishes. The frequencies are evenly spaced: $\omega_i = -1 + 2(i-1)/(N-1)$, $i = 1,\ldots,N$.

Hence, the span of **c** and **s** together with the kernel of **M** account for the whole eigen-space of **M**. The matrix $\mathbf{E}^{-1}\mathbf{M}$ is conjugate to $\mathbf{M}\mathbf{E}^{-1}$, then the linear transformation $\kappa\mathbf{M}\mathbf{E}^{-1}/N$ restricted to two-dimensional subspace formed by **c** and **s** takes the form

$$\frac{\kappa}{N}\mathbf{M}\mathbf{E}^{-1} = \begin{pmatrix} Q_c(\lambda) & Q_a(\lambda) \\ Q_a(\lambda) & Q_s(\lambda) \end{pmatrix}, \tag{21}$$

where the functions $Q_c(\lambda) = \frac{\kappa}{N}\sum_{i=1}^{N}\frac{|\omega_i|c_i^2}{\lambda + \kappa D c_i}$, $Q_s(\lambda) = \frac{\kappa}{N}\sum_{i=1}^{N}\frac{|\omega_i|s_i^2}{\lambda + \kappa D c_i}$ and $Q_a(\lambda) = \frac{\kappa}{N}\sum_{i=1}^{N}\frac{|\omega_i|c_i s_i}{\lambda + \kappa D c_i} = 0$. Therefore, the characteristic polynomial for **J** is

$$p(\lambda) = \det(\mathbf{E})\det\left(\mathbf{I} - \frac{\kappa}{N}\mathbf{E}^{-1}\mathbf{M}\right)\det(\mathbf{W}) = \prod_{i=1}^{N}(\lambda + \kappa D c_i)(1 - Q_c(\lambda))(1 - Q_s(\lambda)). \tag{22}$$

Apart from the poles $-\kappa D c_i$, the functions $Q_c(\lambda)$ and $Q_s(\lambda)$ are strictly decreasing, and so the polynomial $p(\lambda) = 0$ must have exactly two roots ($Q_c(\lambda) = 1$ and $Q_s(\lambda) = 1$) between any two consecutive poles. Obviously, $Q_c(0) = 1$ corresponds to the rotation invariance and the only remaining eigenvalue $Q_s(\lambda) = 1$ determines the stability of the phase-locked state, so the stable condition ($\lambda < 0$) is $Q_s(0) < 1$ which yields

$$\frac{1}{N}\sum_{i=1}^{N}|\omega_i|\frac{s_i^2}{c_i} < D. \tag{23}$$

In the continuous limit, equation (23) is equivalent to the following inequality

$$\int_{\text{lock}} g(\omega)|\omega|\frac{\omega^2}{q^2\sqrt{q^2 - \omega^2}}\mathrm{d}\omega < \frac{1}{\kappa}, \tag{24}$$

which requires $f'(q) < 0$. Therefore, the eigen-spectrum of **J** is made up of three pieces (see figures 2 and 3). The first part, widely distributed in the interval of poles, merges into the continuous spectrum ($-\sqrt{q^2 - \omega^2}$, $q > 1$) as $N \to \infty$. The second part is a trivial eigenvalue $\lambda = 0$ due to the rational symmetry of the Kuramoto model, and the third part is a separated eigenvalue located in between those two, which turns out to be the nontrivial part of the discrete spectrum as $N \to \infty$. For $q \in [1, q_c]$, $f'(q) > 0$, the branch of solution $D(\kappa)$ is unstable, while it is stable for $q \in (q_c, +\infty)$.

To better understand the property of the eigen-spectrum, we concentrate on the continuous limit $N \to \infty$. In this way, the state of the system is described by a real density function $\rho(\theta, \omega, t)$ which satisfies the

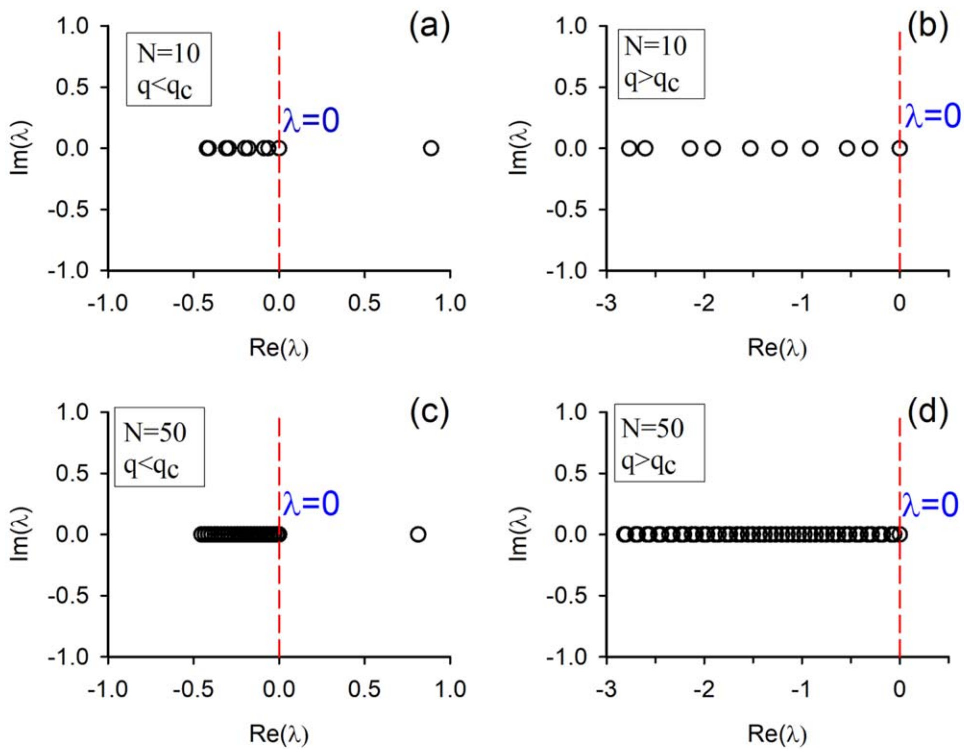

Figure 3. The eigen-spectrum of the Jacobian matrix $\mathbf{J}'$ (see equation (30)). Panels (a) and (c) refer to $q = 1.1$ ($q < q_c$), the largest eigenvalue being $\lambda > 0$. Panels (b) and (d) refer instead to $q = 3.0$ ($q > q_c$), the largest eigenvalue being $\lambda = 0$. The frequencies are evenly spaced: $\omega_i = -1 + 2(i-1)/(N-1)$, $i = 1,\ldots,N$.

normalization condition. Meanwhile, $\rho(\theta, \omega, t)$ is 2π-periodic with respect to θ and can be expanded into Fourier series as

$$\rho(\theta, \omega, t) = \frac{g(\omega)}{2\pi}\sum_{n=-\infty}^{\infty}\alpha_n(\omega, t)e^{in\theta}, \tag{25}$$

where the Fourier coefficients $\alpha_0 = 1$ and $\alpha_{-n} = \alpha_n^*$. Considering the Ott–Antonsen ansatz, $\rho(\theta, \omega, t)$ takes the form of Poisson kernel $\alpha_n = \alpha^n$ [27–30]. Equation (2) is equivalent to the continuous equation

$$\frac{d\alpha}{dt} + i\omega\alpha + \frac{\kappa}{2}(D\alpha^2 - D^*) = 0 \tag{26}$$

with $D(t) = \int_{\text{lock}} g(\omega)|\omega|\alpha^*(\omega, t)d\omega$.

Apart from the incoherent state $\alpha(\omega) = 0$, the phase-locked state $\alpha_0(\omega) = e^{-i\theta(\omega)}$ (see equations (8) and (9)) is another fixed point of equation (26). Linearizing equation (26) around this steady state, one gets

$$\frac{d\delta\alpha}{dt} = -i\omega\delta\alpha - \kappa D\alpha_0\delta\alpha + \frac{i\omega\alpha_0}{D}\delta D = \lambda\delta\alpha. \tag{27}$$

Combining the expression of D with equation (27), the self-consistent equation for λ is

$$1 = \int_{\text{lock}} g(\omega)|\omega|\frac{i\omega\alpha_0/D}{\lambda + i\omega + \kappa D\alpha_0}d\omega. \tag{28}$$

Substituting α_0 into equation (28), the imaginary part vanishes automatically, provided an even $g(\omega)$, and one obtains the eigen-equation for λ

$$1 = \int_{\text{lock}} g(\omega)|\omega|\frac{\omega^2/(\kappa D^2)}{\lambda + \sqrt{(\kappa D)^2 - \omega^2}}d\omega, \tag{29}$$

which is consistent with $Q_s(\lambda) = 1$ in the finite dimensional case. Note that $\lambda = -\sqrt{(\kappa D)^2 - \omega^2}$ just corresponds to continuous spectrum of the linear operator, and the discrete eigenvalue is only determined by equation (29). On the one hand, when κD is large enough, λ must be negative to balance equation (29) (stable solution). On the other hand, when κD is small ($\kappa D \to \max\{\omega\}$), λ should be positive to avoid singularity of equation (29) (unstable solution). As λ is a continuous function of κD, the critical point κ_c and D_c for the emergence of phase-locked state can be obtained by imposing $\lambda \to 0^+$.

The stability analysis for in-coupling case follows a similar procedure, where the Jacobian matrix $\mathbf{J}'$ has the following elements

$$J'_{ij} = \frac{\kappa|\omega_i|}{N}\cos(\theta_i - \theta_j) - \kappa R|\omega_i|\cos\theta_i\delta_{ij}. \tag{30}$$

The eigenvalues of $\mathbf{J}'$ are the roots of $Q'_c(\lambda) = 1$ and $Q'_s(\lambda) = 1$, where $Q'_c(\lambda) = \frac{\kappa}{N}\sum_{i=1}^{N}\frac{\cos^2\theta\,|\,\omega_i\,|}{\lambda + \kappa R\cos\theta\,|\,\omega_i\,|}$ and $Q'_s(\lambda) = \frac{\kappa}{N}\sum_{i=1}^{N}\frac{\sin^2\theta\,|\,\omega_i\,|}{\lambda + \kappa R\cos\theta\,|\,\omega_i\,|}$. The structure of the eigen-spectrum has the same form as equation (22). There are $N - 2$ distinct eigenvalues in the interval $(-\kappa R\cos\theta|\omega_i|, -\kappa R\cos\theta|\omega_{i-1}|)$, $Q'_c(0) = 1$ and the remaining one is determined by $Q'_s(\lambda) = 1$ that yields stable condition $Q'_s(0) < 1$, i.e. $\tan^2\theta < 1$. It is easily checked that the stable condition holds for $\theta(R_+) < \pi/4$, and it is violated since $\theta(R_-) > \pi/4$. We emphasize that in contrast to the out-coupling case, the discrete eigenvalue for R_+ is empty as $N \to \infty$. Since the existence interval $(-\kappa R\cos\theta|\omega_1|, 0)$ for $\lambda(R_+)$ gets shorter and shorter, $|\omega_1| = \min\{\omega_i\}$. Once $|\omega_1| \to 0$, the interval vanishes and λ is absent.

Let us move now to describe the eigenvectors associated to the eigenvalues. The natural frequencies are reordered as $|\omega_1| \geqslant |\omega_2| \geqslant \ldots \geqslant |\omega_N|$ and $\omega_{2i} = -\omega_{2i-1}$. For an even N, $\mathbf{R}^N$ can be split into two subspace V_{even} and V_{odd}, such that $\mathbf{x} \in \mathrm{V}_{\mathrm{even}}$, $x_{2i} = x_{2i-1} (i = 1, 2, \ldots, N/2)$ and $\mathbf{x} \in \mathrm{V}_{\mathrm{odd}}$, $x_{2i} = -x_{2i-1} (i = 1, 2, \ldots, N/2)$. Thus, $\dim(\mathrm{V}_{\mathrm{even}}) = \dim(\mathrm{V}_{\mathrm{odd}}) = N/2$, and $V_{\mathrm{even}} \perp V_{\mathrm{odd}}$, consequently, the vector $\mathbf{c} \in \mathrm{V}_{\mathrm{even}}$ and $\mathbf{s} \in \mathrm{V}_{\mathrm{odd}}$.

If $\mathbf{x} \in \mathrm{V}_{\mathrm{even}}$, then for the out-coupling case

$$\mathbf{J}\mathbf{x} = -\kappa D\mathbf{C}\mathbf{x} + \frac{\kappa}{N}\mathbf{M}\mathbf{W}\mathbf{x} = \lambda\mathbf{x}. \tag{31}$$

If one defines $\mathbf{y} = \mathbf{W}\mathbf{x}$ and $\mathbf{y} \in V_{\mathrm{even}}$, then $\mathbf{y}$ satisfies

$$\mathbf{E}\mathbf{y} = \frac{\kappa}{N}\mathbf{M}\mathbf{y} = \frac{\kappa}{N}(\mathbf{c}\cdot\mathbf{y})\mathbf{c}. \tag{32}$$

Set $\mathbf{c}\cdot\mathbf{y} = N/\kappa$, then $\mathbf{y} = \mathbf{E}^{-1}\mathbf{c}$ and the entry of the eigenvector $x_i = \frac{c_i}{\lambda + \kappa Dc_i}$. Considering the self-consistent condition, the eigenvalue λ for $\mathbf{x} \in V_{\mathrm{even}}$ corresponds to $Q_c(\lambda) = 1$. Furthermore, if $\mathbf{x} \in V_{\mathrm{odd}}$ is the eigenvector of $\mathbf{J}$, then $x_i = \frac{s_i}{\lambda + \kappa Dc_i}$, which implies $Q_s(\lambda) = 1$. Due to $\mathbf{J}$ preserves V_{even} and V_{odd}, the eigenvectors of $\mathbf{J}$ can be understood clearly. The even eigenvector $\mathbf{x}$ corresponds to a purely vertical perturbation to the order parameter. Since the first-order deviation caused by $\mathbf{x}$, $\nabla(D\cos\Theta)\cdot\mathbf{x} = 0$ and $\nabla(D\sin\Theta)\cdot\mathbf{x} \neq 0$. On the other hand, the odd eigenvector $\mathbf{x}$ corresponds to a purely horizonal perturbation to the order parameter because the first-order derivative along this direction is $\nabla(D\cos\Theta)\cdot\mathbf{x} \neq 0$ and $\nabla(D\sin\Theta)\cdot\mathbf{x} = 0$. Similar results occur for the in-coupling case.

4. Tiered phase transition

Figure 4 illustrates the phase diagram of the system by direct numerical simulation with $N = 100\,000$. The blue solid lines are the theoretical predictions indicating stability ($q > q_c$). The green dashed lines represent a branch of unstable solution ($q < q_c$). Both the in- and out-coupling schemes exhibit a similar route to synchronization, namely, a tiered phase transition appears from the incoherent state to the oscillatory state, then to the phase-locked state. For the incoherent state, all oscillators are disordered and distribute uniformly on the unit circle, and two coupling schemes show the same critical point $\kappa_{c,1} = 4\sqrt{2}/\pi$. Interestingly, these two coupling schemes reveal different properties of the coherent state in spite of $N \to \infty$. The critical point $\kappa_{c,2}$ for the emergence of phase-locked state is postponed for the out-coupling case. In this sense, we can say that the whole synchronization ability in the out-coupling case is weaker than the in-coupling case (see figure 4(d)). The differences of synchronization ability between these two cases may provide significant strategies for synchronization optimization in real system.

Figure 5 plots several typical features of the oscillatory state for both cases. In contrast to the metastable state reported in [21], where the system (the order parameter) experiences a long-lasting fluctuation near the critical point of the travelling-wave state (a signature of a hybrid phase transition), here we find that the oscillatory state behaves as a stable periodic-T vibration of the order parameters $Z_{1,2}$ without any fluctuation (figures 5(e) and (f)). In addition, the oscillatory state takes place in a particular regime ($\kappa_{c,1} < \kappa < \kappa_{c,2}$) [31–35], where the incoherent state loses its stability and phase-locked state is empty. As a type of time-dependent clustering state, a number of phases appear locked according to their natural frequencies (see figures 5(a) and (b)). Consequently, the effective frequencies averaged in long time limit correlate in a way that they converge to a common value $\langle\omega_i\rangle = \pm 2\pi/T$ [36] (figures 5(c) and (d)). It should be pointed out that the instantaneous velocities of all oscillators within each group are distinct, which leads to the oscillation of the order parameters [37]. We argue that the onset of such state is related to the Hopf bifurcation in the phase space characterized by nonzero Ω_c, and it disappears at $\kappa_{c,2}$ accompanying saddle-node bifurcation of the phase-locked state.

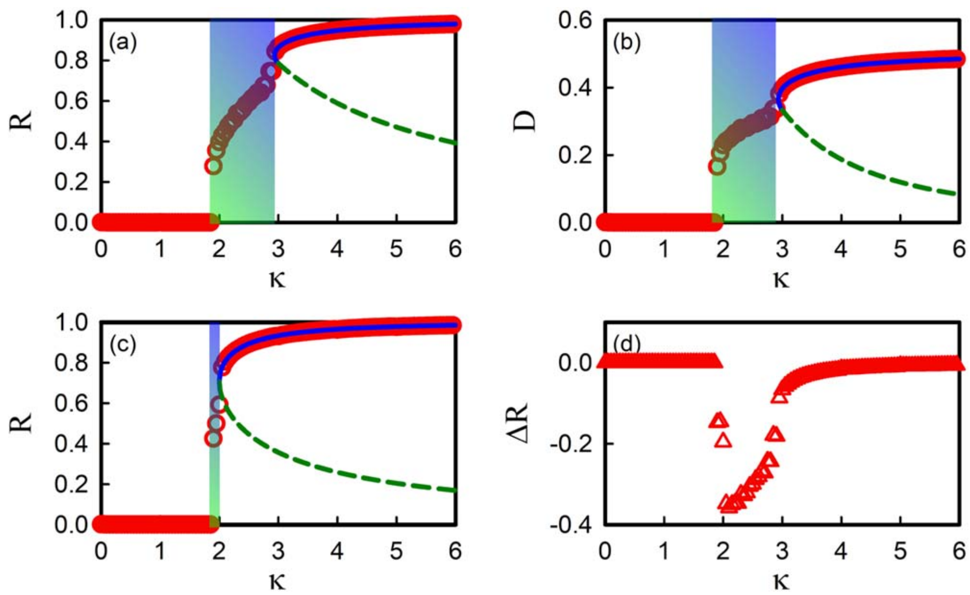

Figure 4. Phase diagrams of the order parameters R, D versus the coupling strength κ. Panels (a) and (b) refer to the out-coupling case, panel (c) refers to the in-coupling case, and panel (d) reports the difference of the order parameters between (a) and (c). The red circles are the results of numerical simulations for $N = 100\,000$, $\Delta t = 0.01$ with a fourth-order Runge–Kutta integration scheme, and the distribution of the natural frequency is uniform (equation (2), $\Delta = 1$). The total running time is $t = 500$ and the order parameters are averaged over the last $\Delta t = 50$. The blue solid lines are the theoretical predictions from self-consistent equations for $q > q_c$, and the green dashed lines refer to the case $q < q_c$. The colourful shadows in (a)–(c) are the regions where the oscillatory state exists.

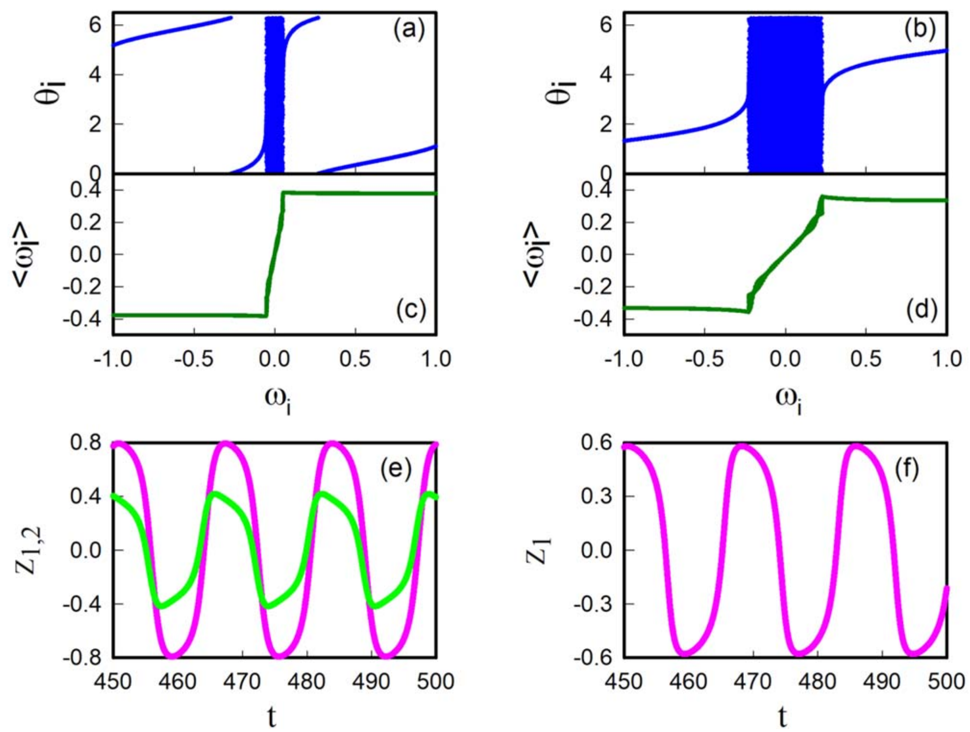

Figure 5. Typical features of the oscillatory state. The left panels refer to the out-coupling case ($\kappa = 2.5$) and the right panels refer to the in-coupling case ($\kappa = 1.9$). Panels (a) and (b) report the instantaneous phases θ_i versus ω_i, while panels (c) and (d) report the effective frequencies $\langle\omega_i\rangle$ versus ω_i. Panels (e) and (f) are time series of the order parameters $Z_{1,2}$, where $Z_{1,2}$ are purely real. Pink represents Z_1 and green represents Z_2.

5. Conclusion

In summary, we extended the Kuramoto model, and accounted for both in- and out-coupling heterogeneity. We reveal a type of universal phase transition from the incoherent state to the phase-locked state via an oscillatory state without any repulsive coupling. The critical points for the occurrence of the coherent states and stable solutions of the phase-locked states are obtained analytically, and the predictions have been perfectly supported by numerical simulations. A simple stable condition for the formation of the phase-locked state is provided in terms of matrix analysis theory, and in full consistency with the Ott–Antonsen analysis in the limit $N \to \infty$. This work not only enhances our understanding of dynamical phase transitions in coupled oscillators with general heterogenous coupling, but also sheds light on synchronization control and optimization.

Acknowledgments

This work is partially supported by the National Natural Science Foundation of China (Grant Nos. 11835003, 11875132, 11905068, 11847013 and 11875135), and the Natural Science Foundation of Shanghai (No. 18ZR1411800), the Scientific Research Funds of Huaqiao University (Grant No. 605-50Y17064), and the Scientific Project Funds of Quanzhou (Grant No. 2018C085R).

ORCID iDs

Shuguang Guan https://orcid.org/0000-0001-8512-371X

References

[1] Pikovsky A, Rosenblum M and Kurths J 2001 *Synchronization: A Universal Concept in Nonlinear Sciences* (Cambridge: Cambridge University Press)
Boccaletti S, Kurths J, Osipov G, Valladares D L and Zhou C S 2012 The synchronization of chaotic systems *Phys. Rep.* **366** 1
Boccaletti S, Pisarchik A N, Del Genio C I and Amann A 2018 *Synchronization: From Coupled Systems to Complex Networks* (Cambridge: Cambridge University Press)
[2] Strogatz S H 2003 *Sync: The Emerging Science of Spontaneous Order* (New York: Hachette Books)
[3] Nishikawa T and Motter A E 2015 Comparative analysis of existing models for power-grid synchronization *New J. Phys.* **17** 015012
[4] Kuramoto Y 1984 *Chemical Oscillations, Waves and Turbulence* (Berlin: Springer) pp 75–6
[5] Winfree A T 1967 Biological rhythms and the behavior of populations of coupled oscillators *J. Theor. Biol.* **16** 15
[6] Kuramoto Y 1975 Self-entrainment of a population of coupled non-linear oscillators *International Symposium on Mathematical Problems in Theoretical Physics* (Berlin: Springer) pp 420–2
[7] Acebrón J A, Bonilla L L, Vicente C J P, Ritort F and Spigler R 2005 The Kuramoto model: a simple paradigm for synchronization phenomena *Rev. Mod. Phys.* **77** 137
[8] Chen B, Engelbrecht J R and Mirollo R 2019 Dynamics of the Kuramoto–Sakaguchi oscillator network with asymmetric order parameter *Chaos* **29** 013126
[9] Gómez-Gardenẽs J *et al* *Phys. Rev. Lett.* **106** 128701
Leyva I *et al* 2012 *Phys. Rev. Lett.* **108** 168702
Leyva I *et al* 2013 *Nat. Sci. Rep.* **3** 1281
Zhang X *et al* 2013 *Phys. Rev.* E **88** 010802(R)
Zhang X, Boccaletti S, Guan S and Liu Z 2015 *Phys. Rev. Lett.* **114** 038701
Boccaletti S *et al* 2016 *Phys. Rep.* **660** 1
[10] Zanette D H 2005 Synchronization and frustration in oscillator networks with attractive and repulsive interactions *Europhys. Lett.* **72** 190
[11] Paissan G H and Zanette D H 2007 Synchronization and clustering of phase oscillators with heterogeneous coupling *Europhys. Lett.* **77** 20001
[12] Bartsch R P, Schumann A Y, Kantelhardt J W, Penzel T and Ivanov P C 2012 Phase transitions in physiologic coupling *Proc. Natl Acad. Sci. USA* **109** 10181–6
[13] Xu L, Chen Z, Hu K, Stanley H E and Ivanov P C 2006 Spurious detection of phase synchronization in coupled nonlinear oscillators *Phys. Rev.* E **73** 065201(R)
[14] Bashan A, Bartsch R P, Kantelhardt J W, Havlin S and Ivanov P C 2012 Network physiology reveals relations between network topology and physiological function *Nat. Commun.* **3** 702
[15] Ivanov P C, Liu K K and Bartsch R P 2016 Focus on the emerging new fields of network physiology and network medicine *New J. Phys.* **18** 100201
[16] Ivanov P C, Liu K K, Lin A and Bartsch R P 2017 *Network Physiology: From Neural Plasticity to Organ Network Interactions (In Emergent Complexity from Nonlinearity, in Physics, Engineering and the Life Sciences)* (Cham.: Springer) pp 145–65
[17] Abrams D M, Mirollo R, Strogatz S H and Wiley D A 2008 Solvable model for chimera states of coupled oscillators *Phys. Rev. Lett.* **101** 084103
[18] Hong H and Strogatz S H 2011 Mechanism of desynchronization in the finite-dimensional kuramoto model *Phys. Rev. Lett.* **106** 054102
[19] Ottino-Löffler B and Strogatz S H 2018 Volcano transition in a solvable model of frustrated oscillators *Phys. Rev. Lett.* **120** 264102
[20] Ji P, Peron T K D M, Menck P J, Rodrigues F A and Kurths J 2013 Cluster explosive synchronization in complex networks *Phys. Rev. Lett.* **110** 218701
[21] Park J and Kahng B 2018 Metastable state en route to traveling-wave synchronization state *Phys. Rev.* E **97** 020203
[22] Xu C, Boccaletti S, Guan S and Zheng Z 2018 Origin of Bellerophon states in globally coupled phase oscillators *Phys. Rev.* E **98** 050202(R)
[23] Sonnenschein B, Peron T K D M, Rodrigues F A, Kurths J and Schimansky-Geier L 2015 Collective dynamics in two populations of noisy oscillators with asymmetric interactions *Phys. Rev.* E **91** 062910
[24] Pazó D 2005 Thermodynamic limit of the first-order phase transition in the Kuramoto model *Phys. Rev.* E **72** 046211

[25] Xu C, Gao J, Xiang H, Jia W, Guan S and Zheng Z 2016 Dynamics of phase oscillators with generalized frequency-weighted coupling *Phys. Rev.* E **94** 062204
[26] Mirollo R E and Strogatz S H 2005 The spectrum of the locked state for the Kuramoto model of coupled oscillators *Physica* D **205** 249–66
[27] Ott E and Antonsen T M 2008 Low dimensional behavior of large systems of globally coupled oscillators *Chaos* **18** 037113
[28] Ott E and Antonsen T M 2009 Long time evolution of phase oscillator systems *Chaos* **19** 023117
[29] Pikovsky A and Rosenblum M 2008 Partially integrable dynamics of hierarchical populations of coupled oscillators *Phys. Rev. Lett.* **101** 264103
[30] Pikovsky A and Rosenblum M 2015 Dynamics of globally coupled oscillators: Progress and perspectives *Chaos* **25** 097616
[31] Martens E A *et al* 2009 Exact results for the Kuramoto model with a bimodal frequency distribution *Phys. Rev.* E **79** 026204
[32] Sakaguchi H 1988 Cooperative phenomena in coupled oscillator systems under external fields *Prog. Theor. Phys.* **79** 39
[33] Montbrió E, Kurths J and Blasius B 2004 Synchronization of two interacting populations of oscillators *Phys. Rev.* E **70** 056125
[34] Wang H and Li X 2011 Synchronization and chimera states of frequency-weighted Kuramotooscillator networks *Phys. Rev.* E **83** 066214
[35] Yuan D, Zhang M and Yang J 2014 Dynamics of the Kuramoto model in the presence of correlation between distributions of frequencies and coupling strengths *Phys. Rev.* E **89** 012910
[36] Engelbrecht J R and Mirollo R 2012 Structure of long-term average frequencies for kuramoto oscillator systems *Phys. Rev. Lett.* **109** 034103
[37] Bi H, Hu X, Boccaletti S, Wang X, Zou Y, Liu Z and Guan S 2016 Coexistence of quantized, time dependent, clusters in globally coupled oscillators *Phys. Rev. Lett.* **117** 204101